

MEASUREMENT OF THE SPATIAL RESPONSE OF A DETECTOR PIXEL

Y. Zabar^{1,2}, E. N. Ribak², and S. G. Lipson²

¹SemiConductor Devices (SCD), P.O. Box 2250, Haifa 31021, Israel

²Department of Physics, Technion – Israel Institute of Technology, Haifa 32000, Israel

ABSTRACT

In order to measure the internal spatial response of a pixel in a detector, it is scanned by a beam smaller than its size. This becomes difficult as the wave length grows and becomes comparable to the pixel size, such as in the infra red. To overcome this difficulty, a special phase mask which makes the beam narrower was designed, constructed, and tested successfully. The mask was made from five alternating transparent rings, where the rings had half a wave phase difference between them. The beam was scanned with and without the mask in two dimensions in fine steps by a much smaller detector and its response was taken. The spot width dropped by 19% at half its height and by 42% at tenth its height, a significant narrowing. The scan was repeated with the full detector pixel. That beam scan served as a deconvolution kernel and allowed us to find the pixel point spread function (spatial response), the pixel modulation transfer function and the optical cross talk between the pixels.

Keywords: PSF, IR detector, super-resolution, phase mask, pixel, spatial response

1. Introduction

The design of pupil filters to overcome the limits in resolution imposed by diffraction in imaging systems has long been the aim of many research efforts. Point spread function (PSF) engineering using pupil filters is currently an active area of research [1-6]. Many pupil filters have been proposed. At first, these filters were based on variable-transmittance pupils [1]. However, in recent years, attention has centered on the design of phase-only profiles. This is due to the fact that, in general, phase-only filters yield better performance than transmittance filters [2]. Many phase profiles that achieve transverse super-resolution are based on annular designs. Diffractive super-resolution elements were proposed by Sales and Morris [3] and, more recently, the three-zone binary phase filters were reported by Wang *et al.* [4], designed to increase the data storage density in the next-generation digital video devices.

A novel procedure for shaping the axial component of the point spread function of non paraxial focusing systems by use of phase-only pupil filters is presented. The procedure is based on Toraldo di Francia's technique for tailoring focused fields [1]. The pupil filters consisted of a number of concentric annular zones with constant real transmittance. The number of zones and their widths were optimized according to the PSF shape requirements. We found that indeed super-resolution improves as the number of annuli increased. Our method was applied to design filters that produce axial super-resolution in a scanning system. The design goal was to create a point-spread function with a small central spot and with distant side lobes that will be blocked in front of the detector or will be small enough or easily separable. The intensity of the central lobe was not an important parameter for our application of pixels spatial response measurements. We wished to test the response of the pixels of an infra red detector, the uniformity inside the pixels and across the pixels. We also wished to measure the optical cross talk between the pixels. The pixel size we were interested in was 20 μ m by 20 μ m, and the test wave length was 4.6-4.8 μ m incoherent light. Since this wave length allows at best approximately 5 by 5 measurement points, we wished to increase the number of points by reducing the beam size. Another use for the special optics is for testing smaller future pixels. Towards this end, we designed a special phase mask, to be inserted in the Fourier plane of the scanning beam.

2. Operating principle of the system

Figure 1 shows the optical system. The collimated light passes through a phase-shifting apodizer and then converges through an objective lens onto the IR detector. From Fraunhofer diffraction [8] we get:

$$U(x, y) = \frac{\exp(jkz) \exp\left[j \frac{k}{2z} (x^2 + y^2)\right]}{j\lambda z} \int_{-\infty}^{\infty} \int_{-\infty}^{\infty} U(\xi, \eta) \exp\left[-j \frac{2\pi}{\lambda z} (x\xi + y\eta)\right] d\xi d\eta \quad (1)$$

While: $z \gg \frac{k(\xi^2 + \eta^2)_{\max}}{2}$

The diffracting aperture is assumed to lie in the (ξ, η) plane, and is illuminated in the positive z direction. The wavefront is calculated across the (x, y) plane, which is parallel to the (ξ, η) plane and at normal distance z from it. The z axis pierces both planes at their origins.

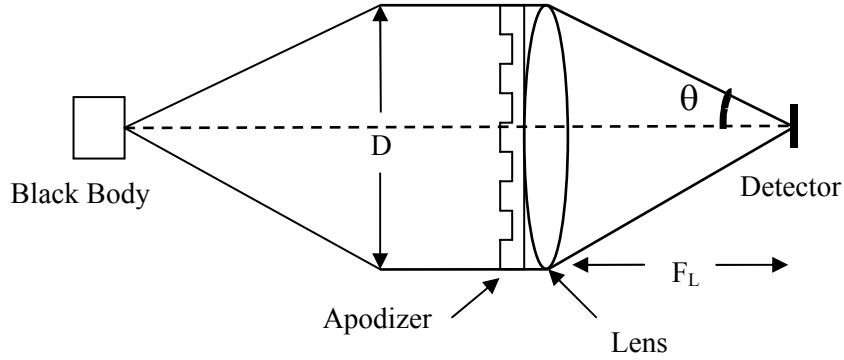


Fig. 1. System setup

For an N -portion annular phase-shifting apodizer, the normalized amplitude distribution in the image side is:

$$U(\rho, u) = 2 \sum_{j=1}^N e^{i\phi_j} \int_{r_{j-1}}^{r_j} r J_0(\rho r) \cdot e^{-0.5iur^2} dr \quad r = \sqrt{(x^2 + y^2)} \quad (2)$$

$$U(\rho, 0) = 2 \sum_{j=1}^N e^{i\phi_j} \int_{r_{j-1}}^{r_j} r J_0(\rho r) dr = \frac{2}{\rho} \sum_{j=1}^N e^{i\phi_j} [r_j J_1(\rho r_j) - r_{j-1} J_1(\rho r_{j-1})]$$

where u is the axial coordinates in the image side, r is the radial coordinates in the image side, ϕ_j is the phase of zone j and ρ is the radial position of each zone. The intensity along the axis is:

$$I(0, u) = |U(0, u)|^2 \quad (3)$$

and in the image plane is:

$$I(\rho, 0) = |U(\rho, 0)|^2 \quad (4)$$

The mask (Figure 2) was made from five alternating transparent rings of ZnS, where the rings had a π phase difference between them at the central wave length. The diameters of the rings were calculated according to an optimization scheme, which required a minimum central beam diameter, and side lobes which were to be as distant as possible and have minimum intensity. Another constraint was a 10% band width, and we tried different initial conditions and different number of rings. These side lobes were not blocked and were able to reach the final detector, but only on neighboring pixels. The design was copied into a transparent and opaque mask, which in turn was then reduced onto the phase mask for etching.

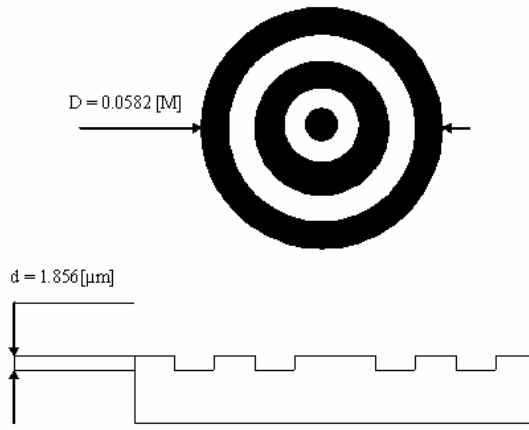


Fig. 2. Structure of the phase mask

The depth of etching was calculated from the phase difference:

$$\Delta\phi = \phi_2 - \phi_1 = \frac{2\pi nd}{\lambda} - \frac{2\pi d}{\lambda} = \frac{2\pi(n-1)d}{\lambda} = \pi$$

$$\Rightarrow d = \frac{\lambda}{2(n-1)} \quad (5)$$

where ϕ_1 is the phase gained while passing throughout the air, ϕ_2 is the phase gained while passing throughout the material, and n is the refraction index of the ZnS [7].

3. Measurements and numerical results

The method for measuring the spatial response of a detector (designated detector PSF), is a 2D spot scan and included two stages. In the first stage we characterized the beam and the optical setup. By using a small sampling diode we scanned the beam and found its response (the setup PSF). The actual setup PSF was found after deconvolution between the measured beam and the sampling diode. In the second stage we characterized the detector (pitch of 20 μm) and found the detector PSF after deconvolution with the actual beam profile (the setup PSF). The PSF measurement algorithm is illustrated in Fig. 3:

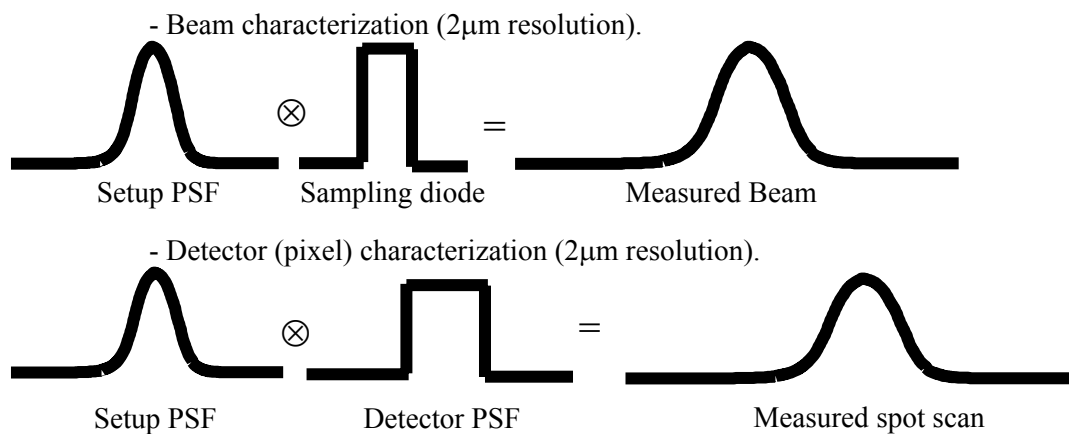


Fig. 3. Detector PSF measurement algorithm

The beam characterization was performed using a 4 μm by 4 μm PV-MCT test diode in front illumination with a narrow-band filter of $\lambda=4.6\text{-}4.8\mu\text{m}$ and $F\# = 1$ using AC detection from lock-in-amplifier. The detector was placed on X, Y, Z stages and the beam was scanned at 2 μm steps in two dimensions covering 50 μm by 50 μm and its response was taken with and without the phase mask (Figure 4). The spot width dropped by 19% at half its height and by 42% at tenth its height, a significant narrowing. Moreover, even a depth error of 20 μm did not render

it much wider, and had a fringe benefit: at a slight focus error, the side lobes were smeared and their magnitude was less than 8% of the central peak, even lower than their calculated value. The maximum intensity of the spot with mask was five times lower than the intensity without mask. That was the first stage in which we characterized the beam and the optical setup.

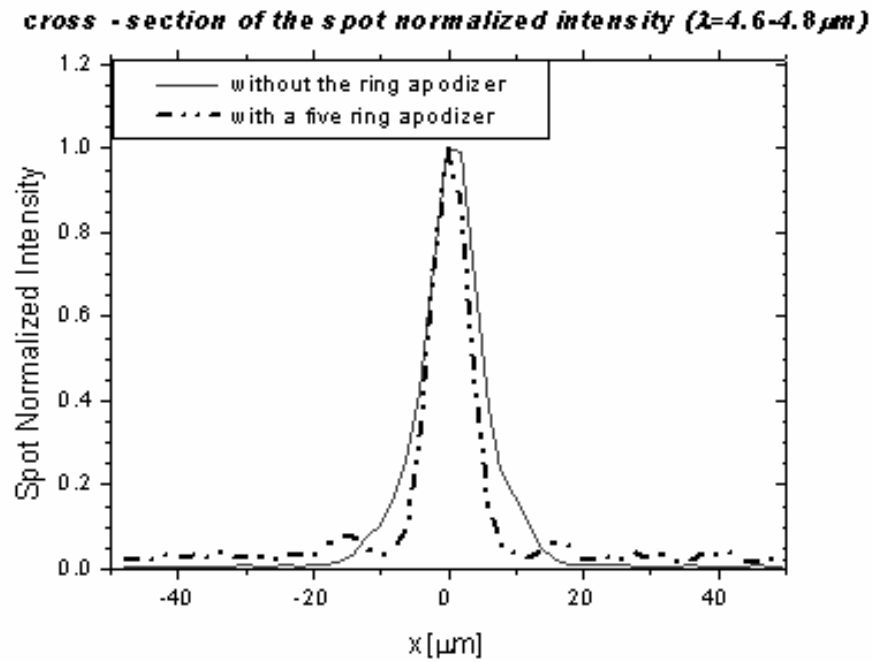


Fig. 4. Beam characterization results (setup PSF)

In the second stage, an InSb detector (back illuminated) at 77K inside a dewar was scanned at 2 μm steps in two dimensions, covering 140 μm by 140 μm and its response was taken. The field stop of the 512 by 640 pixels detector inside the dewar had $f\# < 1$ so the $f\#$ was determined by the optical setup to be one. The measurement conditions included ten frames averaging in every step and a filter with wave length of 4.6μm - 4.8μm. The sampling was performed by the detector processor and A/D setup, and the Black Body source temperature was 650C. The setup PSF (Fig.4, dashed line) served as a deconvolution kernel and allowed us to find the pixel PSF (spatial response) shown in Figure 5. We found that the pixel PSF had a square shape and its dimensions were as expected.

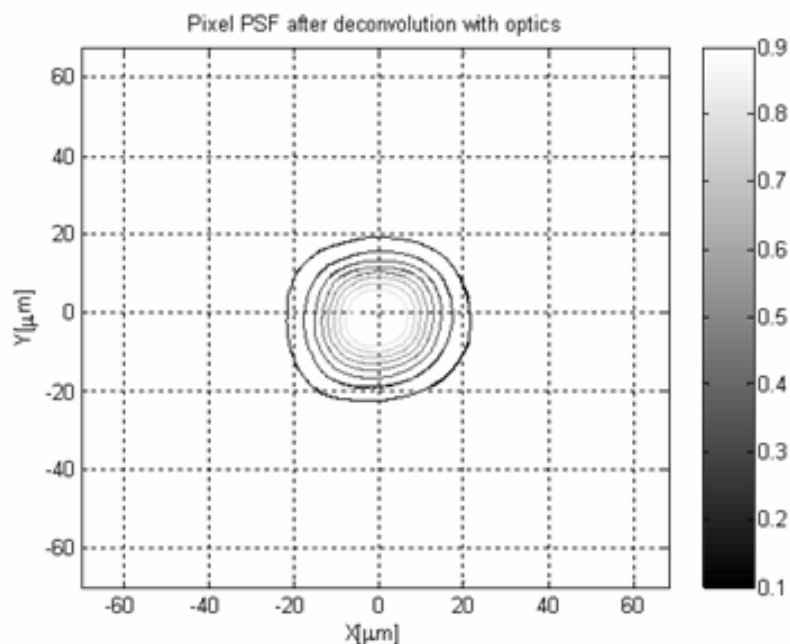


Fig. 5. Pixel PSF measurement results

4. Summary & Conclusion

Super-resolution is the ability to resolve past the classical limit. Pupil plane filters provide a way to do this - in particular phase only filters. Super-resolution appears to improve as the number of annuli is increased. There is large scope for applications of filters: confocal microscopy - scanning resolution and controlled depth of scanning, optical data storage, optical lithography and astronomy. Production is now much easier than ten years ago and so super-resolution methods may be used for many other applications. The design of the phase mask presented in this work is unique and more complicated because the source is not a laser and has a 4% band width. The system is planned for mid-IR radiation - a fact which restricts us to work with unique materials and not the conventional glass materials.

The phase mask that was added to the system reduced the spot size of the source significantly. The spot width dropped by 19% at half its height and by 42% at tenth its height. A depth error of 20 μm did not render it much wider, and at a slight focus error, the side lobes were smeared and their magnitude was less than 8% of the central peak, even lower than their calculated value. The peak intensity of the spot with mask was five times lower than the intensity without mask. A 20 μm detector was scanned and after a deconvolution with the PSF of the optical setup, the PSF of the pixel was found. From the PSF of the pixel, the MTF and cross talk of the detector were calculated. In the future, with smaller pixels, PSF measurements with the phase mask might be even more important for improvement of the measurement accuracy.

5. Acknowledgements

This research was funded by SCD and took place in SCD laboratories. We would like to thank the people in SCD that helped in the production of the phase mask, the optical setup and the measurements.

6. References

1. G. Toraldo di Francia, *Nuovo Cimento Suppl.* **9**, 426 – 438 (1952).
2. T. R. M. Sales and G. M. Morris, "fundamental limits of optical superresolution ", *Opt. Lett.* **22**, 582- 584 (1997).
3. T. R. M. Sales and G. M. Morris, "Diffractive superresolution elements", *J. Opt. Soc. Am. A* **14**, 1637- 1646 (1997).
4. Haifeng Wang and Fuxi Gan, "High focal depth with a pure phase apodizer", *Appl. Opt.* **40**, 5658-5662 (2001).
5. M. Martinez-Corral and M. T. Caballero, "Tailoring the axial shape of the point spread function using the Toraldo concept", *Opt. Exp.* **10**, 98-103 (2002).
6. H. Ando, "phase- shifting apodizer of three or more portions", *Jpn. J. Appl. Phys.* **31**, 557-567 (1992).
7. T.M. Bieniewski and S.J.Czyzak, *Refractive Indexes of Single Hexagonal ZnS and CdS Crystals* *J. Opt. Soc. Am.* **53**, 496 (1963).
8. Joseph. W. Goodman, *Introduction to Fourier optics*, 2nd ed. McGraw Hill (1996)